

Energetic Stability and Magnetic moment of Tri-, Tetra-, and Octa- Ferromagnetic Element nitrides Predicted by First-Principle Calculations.

Yoji Imai^{1,2}, Mitsugu Sohma¹, Takashi Suemasu²

¹ National Institute of Advanced Industrial Science and Technology,

AIST Tsukuba Central 5, Higashi 1-1 Tsukuba, Ibaraki 305-8565, Japan

² Institute of Applied Physics, University of Tsukuba,

1-1-1 Tennohdai, Tsukuba, Ibaraki 305-8573, Japan

Abstract

Formation energies and magnetic moments of tri-, tetra-, and octa- ferromagnetic element nitrides have been calculated using spin-polarized Perdew-Wang generalized gradient approximations of the density functional theory. From the energetic point of view, Fe₄N are more stable compared to Fe and N₂ gas. Ni₄N may be a metastable phase since mixture of Ni₃N and Ni would be more stable. Co₄N are not stable compared to Co metal with the hcp structure and N₂ gas, but stable if compared to Co metal with the fcc structure. Only Fe₈N with the α'-Fe₁₆N₂ type structure would be stable among octa-metal nitrides with the assumed structure of the α'-Fe₁₆N₂ type and the Ni₃₂N₄-type structure. All of Fe₃N, Co₃N, and Ni₃N are stable, but Ni₃N would be paramagnetic in contrast to ferromagnetism of other tri-metal nitrides.

Key Words; Fe₄N, Fe₁₆N₂, Co₄N, Ni₄N, Fe₃N, Co₃N, Ni₃N

1. Introduction

Some of transition metal (TM) compounds with non-metallic (NM) elements whose stoichiometric ratios of TM to NM are high are composed of TM atoms with the face-centered-cubic (fcc), hexagonal closed packed (hcp), or body-centered cubic (bcc) lattice and NM atoms which occupy regularly their interstitial sites.

For example, all of the tetra magnetic element nitrides (Me_4N : Me = Fe, Co, or Ni, N, nitrogen) have the same crystal structure, usually referred to as anti-perovskite structure with the space group $P\bar{m}3m$. Metal atoms are arranged in the fcc structure and nitrogen atoms occupy the body center positions of the metal fcc cells. Relatively large magnetic moment of Fe_4N and relatively high spin-polarization ratio predicted for Co_4N [1] are attractive natures of these compounds, though Co_4N has not been successfully prepared by conventional chemical processes such as thermal decomposition of metal ammine azides. It has been prepared by inequilibrium process such as reactive sputtering [2].

In addition, octa-ferromagnetic 3d element nitrides (Me_8N) is found for Fe_8N , where interstitial octahedral positions of a $2 \times 2 \times 2$ supercell of α -Fe with the bcc structures are occupied by two N atoms. This compound is usually referred to as α "- Fe_{16}N_2 and attracted much attention because of its high magnetic moment. This has a body-centered tetragonal symmetry and belong to the space Group of $I4/mmm$ (No.87). However, there have been no reports on the related compounds of other magnetic elements. Though formation of Ni_{32}N_4 was reported [3] where one N atoms located at the body center and three N atoms at the edge centers of a $2 \times 2 \times 2$ supercell of Ni_4N , the relative stability of this structure compared to the possible α "- Fe_{16}N_2 type structure has not been clarified.

Furthermore, there also exist compounds corresponding to tri-metal nitrides (Me_3N), but the crystal structures and the stability of which have not been understood thoroughly. Details of the observed results so far will be given later.

In the present paper, we will report the results of energetic study on the formation of tri-, tetra-, and octa- magnetic element nitrides (i.e. Fe_3N , Co_3N , and Ni_3N ; Fe_4N , Co_4N , and Ni_4N ; Fe_8N , Co_8N , and Ni_8N) so as to evaluate the energetic stability of these compounds.

2. Calculation Method

Calculations have been done using CASTEP (CAmbride Serial Total Energy Package), a first-principle pseudopotential method based on the density-functional theory (DFT) [4] for describing the electron-electron interaction, a pseudopotential

description of the electron-core interaction, and a plane-wave expansion of the wavefunctions, developed by Payne et al [5]. As for the method of approximation to the exchange-correlation term of the DFT, we used spin-polarized Perdew-Wang Generalized Gradient Approximations [6]. The pseudopotential used is the ultrasoft pseudopotential generated by the scheme of Vanderbilt [7] but is accompanied with the non-linear correction [8, 9] so as to treat the local spin density dependence of the exchange and correlation energy. Wavefunctions were expanded by plane-waves where the number of plane-wave-expansion was set so as to correspond to a kinetic cutoff energy of 340 eV. As for the k-points sampling for the total energy calculation, the Monkhorst-Packe scheme [10] with the mesh parameter corresponding to the spacing of 0.5 nm^{-1} in the Brillouin zone.

Self-consistent iteration convergence was assumed when the total energy difference between successive cycles was less than 0.001eV per atom. Therefore, the numerical values of calculated energy may have errors ca. $\pm 0.025 \text{ eV}$ per formula unit at most, if we consider the number of atoms in the calculated cell stated later.

The electronic density states (DOS) curves were obtained by broadening the discrete energy levels using a Gaussian smearing function of 0.07 eV full-width at half-maximum (FWHM) on a grid of k-points generated above. The energies are shifted so that the Fermi energies (E_F 's) are aligned with zero.

3. Structures of Compounds

The crystal structures of tetra-metal nitrides and octa-metal nitrides have been well-determined as stated in the Introduction section. Though the $\alpha\text{-Fe}_{16}\text{N}_2$ type structure can be reduced to Fe_8N , calculated shearing stress components such as $\tau_{xy}, \tau_{yz}, \dots$ are large and algorithm for geometrical optimization did not work well for this reduced structure. Therefore, optimization procedure have been applied to the original structure, where normal stresses are determining factors of the total stress, and not to the reduced structure. As for the Ni_{32}N_4 type structure, optimization calculations have been performed for the reduced structure with the cell composition of Me_8N_1 .

On the other hand, the range of stability and the crystal structure of tri-metal nitrides have not been thoroughly investigated. The existence of ϵ -phase, belonging to the space group of P 63/mmc (No.194), in the Fe-N system has been confirmed and this is believed to be an interstitial alloy where Fe atoms are arranged in a hcp lattice and N atoms occupy part of its octahedral interstitial sites. Since the observed range of composition of this phase in the Fe-N system is from about 26 at% to about 33 at% N at room temperature [11], ϵ -phase in the Fe-N system is sometimes described as

Fe_{3-v}N.

In contrast to the Fe-N system, the range of stability of Ni₃N in the Ni-N system is not known, though Wriedt represented the formation of hexagonal nitride with the assumed formula of Ni₃N [12]. The atomic arrangement of this phase was determined by Villars and Calvert [13] using Juza and Sachsze's data [14] and they concluded that the structure of Ni₃N is the same with one of higher pressure phases of ReO₃. This structure can be regarded as an interstitial alloy where Ni atoms are arranged in an hcp lattice and N atoms occupy part of its octahedral interstitial sites, as stated later Co₃N was also prepared by nitridation of cobalt metal and cobalt fluoride by Juza and Sachsze [15] and it was confirmed that metal atom lattice has a hexagonal symmetry, however, arrangement of N atoms is not determined to our knowledge.

It should be noted that the structures of ϵ -Fe_{3-v}N and Ni₃N are closely related in that metal atoms compose the hcp lattice whose octahedral interstitial sites are partly occupied by N. Fig.1 shows the relation of octahedral interstitial sites in the hcp lattice and the atomic arrangement of Ni₃N with the ReO₃ type structure. In case the octahedral interstitial sites of hcp lattice of Me are fully occupied by N, the compound has the crystal formula of Me₆N₆. If two of six interstitial sites, selected as shown in (b), are fully occupied and other four sites are unoccupied, the crystal formula is Me₆N₂, which is just the case of Ni₃N. ϵ -Fe_{3-v}N which appears in the Fe-N system has the structure where nearly one-third of the octahedral interstitial sites of hcp lattice are occupied by N. Wide range of stoichiometry suggests that selectivity of occupied sites seems not so strong compared to the case of the Ni-N system.

In the present calculations, we assumed, for simplicity, that all the tri-metal nitrides have the Ni₃N type structure. That is, randomness of site occupancy of interstitial sites of metal lattice with hcp structure was disregarded.

We have also performed calculations for nitrogen gas molecule (N₂), iron (Fe), cobalt (Co) and nickel (Ni) metal as a reference state. For N₂, two nitrogen atoms were placed in an empty cube whose side length is 0.3755 nm¹, with assumed distance (d) apart from each other. Electronic energy calculations as a function of d have been performed so as to determine the optimized atomic distance within the N₂ molecule.

¹ This value is selected as the same with the lattice constant of the optimized Ni₄N. The larger the assumed empty cell is, the better approximation to the isolated N₂ molecule can be expected. However, too large empty cell causes difficulty for securing the same calculation conditions of the cut-off energy of plane-wave expansion and k-point sampling spacing of the Brillouin zone because of the computational resources used.

4. Results and Discussion

4.1. Results for reference states of Fe, Co, Ni and N₂

We first briefly describe the optimization results of N₂ (gas), Fe (metal), Co (metal) and Ni (metal). Their optimized lattice constants (or a , inter-atomic distance) are given in the 2nd column of Table 1², compared with observed values shown in brackets, [a_{obs}].

The calculated electronic energies of their unit cells corresponding to their optimized structures are also listed in the 4th column and those per atom are in the last columns. As is clearly seen, Fe with the ferromagnetic bcc structure has the most negative energy, which agrees to the experimental observations, as is previously studied by Asada and Terakura [16]. Ferromagnetic fcc structure and non-magnetic fcc structure have nearly the same energy with one another, though cell volume of magnetic phase is much larger than that of non-magnetic phase due to magnetovolumetric effect. Nonmagnetic hcp structure has the more negative energy than ferromagnetic and non-magnetic fcc structure.

As for cobalt, both fcc and hcp ferromagnetic structures have more negative energies than corresponding nonmagnetic structures, not listed here, but hcp phase is more negative than fcc phase. Lattice constant are slightly overestimated for Co and Ni with their equilibrium structure, while underestimated for Fe. As for N₂ gas, optimized inter-atomic distance is about 5% larger than the observed one.

Therefore, the energy differences between the observed and optimized structures may depend on the chemical species, though we have no comments over the reason at present. However, we use these values as the energies of reference states, hereafter.

4.2. Formation energy calculations of nitrides

At first, we calculated the energies of tetra- ferromagnetic 3d element (Fe, Co, and Ni) nitrides (Me₄N; Me = Fe, Co, or Ni). Calculated energies of optimized Me₄N are shown in the 4th column of Table 2 along with the optimized lattice constants in the 2nd column. We can see again that the lattice constants are slightly overestimated for Co₄N and Ni₄N compared with their observed values, while is underestimated for Fe₄N.

From the calculated electronic energies of Me₄N, Me, and N₂ gas, we can obtain energies of formation of Me₄N, as follows: For example,

$$(-3745.5480) - 4 \times (-868.1636) - (-271.9986) = -0.8949 \text{ eV}$$

represents the formation energy of Fe₄N from the reference states, four Fe atoms in the

² In Table1 (and Tables 2-4), calculated magnetic moments per 3d metal atom are also listed, which will be referred later in Section 4.3).

metallic state with the bcc structure and one N atom in the gaseous molecule.

Calculated formation energies of Fe₄N, Co₄N, and Ni₄N are listed in the 5th column of Table 2.

As shown there, Fe₄N is predicted to be energetically more stable than Fe metal and N₂ gas. Therefore, Fe₄N would be formed by nitridation of Fe metal. In fact, Fe₄N can be synthesized by various methods such as thermal ammonolysis, reactive magnetron sputtering, plasma nitriding, ball milling, chemical vapor deposition, iron implantation, laser nitriding, and so on. Though higher temperature than 773 K is usually required in the nitridation process, nitridation at a low temperature of 548 K has been reported where amorphous iron is used as a precursor [17].

As for Ni₄N, it is also predicted to be energetically more stable than Ni metal and N₂ gas. Though direct nitridation of Ni has not been reported to our knowledge, Ni₄N can be deposited through direct liquid injection CVD using nickelamidinate in NH₃ or NH₃+H₂ at 430 to 470 K [18].

As for Co₄N, it is predicted to be energetically unstable if compared with equilibrium α phase (hcp). Since it has been known that thin film can be deposited from cobalt amidinate on fcc-copper substrate under the existence of NH₃ and H₂ at substrate temperatures from 373 K to 453 K [19]³, present result may seem to be contradictory. However, it is also known that Co₄N exhibits a stepwise decomposition with increasing the elevated temperature [20], perhaps reflecting the instability compared to hcp Co and N₂. Thin film growth of Co₄N on Cu substrate may be due to low mismatch of Co₄N with Cu, as is suggested [19], and not due to energetic stability of Co₄N compared to Co metal with the hcp structure and N₂. It should be also noted that calculations shows Co₄N has a negative formation energy of -0.03 eV in case fcc Co (β phase) is adopted as a reference. That is, the energy change of



is $(-4458.8265) - 4 \times (-1046.6993) - (1/2)(-543.9973) = -0.0307$ eV.

Next, we calculated the energies of octa- ferromagnetic 3d element (Fe, Co, and Ni) nitrides (Me₈N (Me= Fe, Co, or Ni)). As stated above, there are two possible structures for Me₈N; One is a body-centered tetragonal type which has been found for Fe₁₆N₂, and the other is a face-centered cubic structure which has been found for Ni₃₂N₄. Therefore, we performed optimization procedure for both of structures for all of Me₈N.

Calculated energies and magnetic moments of Me₈N are shown in the 4th and 3rd

³ In the absence of H₂, the reaction between Co precursor and NH₃ yields the Co₃N phase.

columns of Table 3, respectively, along with the optimized lattice constants shown in the 2nd column. Here, calculations for $\text{Me}_{32}\text{Si}_4$ with the face-centered cubic structure have been performed for reduced Me_8N_1 , while those for Me_{16}N_2 with the body-centered tetragonal structure have been performed for non-reduced Me_{16}N_2 and not for reduced Me_8N_1 , since non-diagonal components of calculated stress tensor is not trivial in this structure which made convergence procedure to the optimized structures very difficult as already stated in the Method section.

As shown in the 5th column of Table 3, the formation energy of the compounds from metal and N_2 gas, the body-centered tetragonal structure is more stable than face-centered cubic structure in all the cases considered here, and only Fe_8N_1 is predicted to be more stable than coexisting metal and N_2 gas. This agrees to the experimentally observed fact in Fe-N system, but does not for Ni-N system. Perhaps, this is caused by lattice matching since Ni_8N with face-centered cubic structure is formed by exposure of Ni film to N^+ ions in nitrogen ion implantation process.

Thirdly, we calculated the energy of tri-ferromagnetic 3d element (Fe, Co, and Ni) nitrides. As stated above, there is some uncertainty about the structure and composition of tri-metal nitrides, we assumed that all have the Ni_3N type structure. Randomness of site occupancy of interstitial sites of metal lattice with hcp structure will contribute to the stability through configurational entropy, but atomic configuration of the Ni_3N type structure must be favorable from the energetic point of view.

Calculated energies are given in Table 5.

All the calculated data so far are summarized in Fig.2, which shows the variation of formation energy of each compound with the atomic composition. Calculated energy changes for the reaction (1) are visualized in Fig.1 as a function of X. In the Figure open circles, closed triangulars, and open squares denote the Co, Ni, and Fe compounds. Here, energies for octa-metal nitrides are those for the Fe_{16}N_2 type structure, since octa-metal nitrides with the Ni_{16}N_2 type structure has more positive energy of formation compared with those with the Fe_{16}N_2 type structure.

As is shown, Fe-nitrides have the most negative formation energies, followed by Ni nitrides. The reason why the order of stability of nitrides is not the same with (or, reverse to) the order of atomic number is unclear. From the view point of electronegativity, Fe is the most positive (1.83 by Pauling's scale), followed by Co (1.88), then Ni (1.91). Since the electronegativity of N is 3.04, bonding between metal atom and nitrogen seems to be rather covalent with partial ionicity and the affinity between metal and nitrogen must be the largest in Fe-N, followed by Co-N, then Ni-N. Cohesive energy of metallic states is 4.28 eV for Fe, 4.35 eV for Co, and 4.44 eV for Ni.

These factors seem to cause the highest stability of Fe nitride, then followed by Co nitrides. Atomic diameter of Fe, Co, and Ni are 0.117 nm, 0.116 nm, and 0.115 nm, respectively, and volumetric effect for interstitial occupancy will also be favorable for Fe, then Co. Therefore, reasons for non-simple relation between the formation energy and atomic number are left for further considerations.

Among the octa-metal nitrides considered here, only Fe₈N is energetically stable. This result agrees to the fact that only Fe₈N is obtained experimentally by high-temperature processes, though Ni₈N has been found by inequilibrium process such as N ion implantation [2].

As for tetra-metal nitrides, Fe₄N and Ni₄N have negative formation energies⁴, while Co₄N has positive value, though Co₄N will has a negative formation energy of -0.03eV in case fcc Co is adopted as stated above.

As for tri-nitrides, all of Fe₃N, Ni₃N, and Co₃N with the assumed Ni₃N type structure are quite stable.

4.3 Spin-Polarized Density of States and Magnetic Moments

Fig.3 shows the calculated spin-polarized density of states (DOS) of Fe, Fe₈N (Fe₁₆N₂), Fe₄N, and Fe₃N (Fe₆N₂). As is shown, there is a steep peak of DOS for majority spin just below the Fermi level and a steep peak of DOS for minority spin just above the Fermi level for pure Fe. Calculated spin polarization between these two peaks are 2.86 eV.

As N content in the compounds increase, these peaks become a bit broader and spin-polarization between majority spin states and minority spin states (SP) become narrower. SP values for Fe₁₆N₂, Fe₄N and Fe₆N₂ were 2.86 eV, 2.62 eV, and 1.67eV, respectively. Calculated magnetic moments were 2.31 μ_B for Fe, 38.20 μ_B for Fe₁₆N₂, 9.56 μ_B for Fe₄N, and 12.26 μ_B for Fe₆N₂, as listed in Tables 1-4. The calculated value for Fe₄N is close to the observed ones [21].

Magnetic moments per 3d-element atom of these and other compounds are shown

⁴ It should be noted here that negative formation energy of a certain compound does not always means this compound is energetically stable phase, since phase separation from one-phase state into two-phase states may occur. For example, Ni₄N may separate into the mixture of Ni and Ni₃N since the formation energy of Ni₄N is located above the connecting dashed line between the Ni and Ni₃N that means the average formation energy of Ni and Ni₃N. Therefore, Ni₄N is predicted to be energetically unstable compared to the mixture of Ni and Ni₃N. Ni₄N seems to be metastable phase.

in Fig. 4.

Generally, increase in the atomic composition of N causes decrease in the magnetic moments per 3d-atom. However, Fe_4N and Fe_{16}N_2 have higher magnetic moments than pure Fe.

It is supposed that narrowing of the band width due to the expansion of the interatomic distance in Fe_4N , compared to the hypothetical fcc Fe, causes the increase in the itinerancy of conduction electrons through supplying hopping site for electrons, resulting in the broadening of band width and in turn suppresses the increase of exchange-splitting, compared to the case of hypothetical fcc Fe ($2.57 \mu_B$) to $2.39 \mu_B$ for Fe_4N , though still larger than bcc Fe ($2.31 \mu_B$) [22]. However, relatively large values of Fe_{16}N_2 , analogous to bcc structure, seems to be explained by other mechanism⁵.

As for Co and Ni, increase in magnetic moments by introduction of N atom will not be expected, though Co_4N may have slightly higher magnetic moment than hypothetical Co_{16}N_2 . Ni_4N (and hypothetical Ni_{16}N_2) will be also ferromagnetic but Ni_{16}N_2 will not.

5. Conclusions

Formation energies and magnetic moments of tri-, tetra-, and octa-ferromagnetic element nitrides have been calculated using spin-polarized Perdew-Wang generalized gradient approximations of the density functional theory and it is concluded from the energetic point of view that,

- (1) Fe_4N with the anti-perovskite structure are more stable compared to Fe and N_2 gas.
- (2) Ni_4N are also more stable compared to Ni and N_2 gas, but is a metastable phase since mixture of Ni_3N and Ni would be more stable.
- (3) Co_4N are not stable compared to Co metal with hcp structure and N_2 gas, but it is more stable than Co with fcc structure and N_2 .
- (4) Only Fe_8N with the α - Fe_{16}N_2 type structure would be stable among octa-metal nitrides with the assumed structure of the α - Fe_{16}N_2 type and the Ni_{32}N_4 -type structure.
- (5) Fe_3N and Co_3N are ferromagnetic but Ni_3N would be paramagnetic.

⁵ It should be noted that there has been still a question left on giant magnetic moment in Fe_{16}N_2 [23].

References

- [1] Y. Takahashi, Y. Imai, T. Kumagai, *J. Magn. Magn. Mat* 323 (2011) 2941-2944
- [2] J. S. Fang, L. C. Yang, C. S. Hsu, G. S. Chen, Y. W. Lin, G. S. Chen,
J. Vac. Sci. Technol. A 22 (2004) 698-704
- [3] I. M. Neklyudov, A. N. Morozov, *Physica M350* (2004) 325-337
- [4] W. Kohn, L.J. Sham, *Phys. Rev.* 140 (1965) 1133.
- [5] M.C. Payne, M.P. Teter, D.C. Allan, T.A. Arias, J.D. Joannopoulos, *Rev. Modern Phys.* 64 (1992) 1045-1097.
- [6] J. D. Perdew, Y. Wang. *Phys. Rev. B* 45 (1992) 13244-13249.
- [7] D. Vanderbilt, *Phys. Rev. B* 41 (1990) 7892-7895.
- [8] S. G. Louie, S. Froyen, M. L. Cohen, *Phys. Rev. B* 26 (1982) 1738-1742.
- [9] E. G. Moroni, G. Kresse, J. Hafner, *Phys. Rev. B* 56 (1997) 15629-15646.
- [10] H. J. Monkhorst, J. D. Pack, *Phys. Rev. B* 13 (1976) 5188-5192.
- [11] H. A. Wriedt, N. A. Gokcen, R. H. Nafziger, *Bull. Alloy Phase Diagrams*, 8 (1987) 355-377.
- [12] H. A. Wriedt, *Bull. Alloy Phase Diagrams*, 6 (1985) 558- .
- [13] P. Villars, L. D. Calvert, *Peason's Handbook of Crystallographic Data for Intermetallic Phases*, 2nd Ed., Volume 4 (1991), ASM International, The Materials Information Society
- [14] R. Juza, W. Sachsze, *Zeit. Anorg. Allg. Chemie*, 251 (1943) 201-212.
- [15] R. Juza, W. Sachsze, *Z. Anorg. Chem.*, 253(1945) 95-108
- [16] T. Asada, K. Terakura, *Phys. Rev. B* 46 (1992) 13599-13602.
- [17] Yi Han, H. Wang, M. Zhang, M. Su, W. Li, K. Tao, *Inorg. Chem.*, 47 (2008) 1261-1263
- [18] Z. Li, R. G. Gordon, V. Pallem, H. Li, D.V. Shenai, *Chem. Mater.*, 22 (2010) 3060-3066
- [19] H. B. Bhandari, J. Yang, H. Kim, Y. Lin, R. G. Gordon, Q. M. Wang, J. M. Lehn, H. Li, D. Shenai, *ElectroChemical Society J. Solid State Sci. Technol.*, 1 (2012) N79-N84,
- [20] J. S. Fang, L. C. Yang, C. S. Hsu, G. S. Chen, Y. W.; Lin, G. S. Chen,
J. Vac. Sci. Technol., A22 (2004) 698 - 704.
- [21] E. L. P. Blanca, J. Desimoni, N. E. Christensen, H. Emmerich,
S. Cottenier, *Phys. Status Solidi B* 246 (2009) 909-928.
- [22] A. Sakuma, *J. Phys. Soc. Jpn* 60 (1991) 2007-2012
- [23] J. M. Cadogan, *Aust. J. Phys.* 50 (1997) 1093-1192

List of Tables and Figures

Fig.1 Location of octahedral interstitial sites in the hexagonal closed packed (hcp) structure, (a), and the atomic arrangement of Ni₃N with the ReO₃ type structure, assumed by Villars and Calvert [13], (b).

Fig.2 Variation of formation energy of Me_xN_{1-x} (Me: Fe, Co and Ni) with the composition.

Straight lines connecting between compounds have no physical meaning but are drawn so as to be easily viewable. However, the dashed line connecting X=0.0 (pure metal) and Ni₃N means the variation of average formation energy when pure Ni and Ni₃N coexist.

Fig.3 Spin-polarized electronic density of states of Fe, Fe₈N, Fe₄N, and Fe₃N.

The upper half indicates the majority spin state and the lower half is for the minority spin state. The energies are shifted so that the Fermi energies (E_F's) are aligned with zero.

Fig.4 Variation of magnetic moment per atom (Fe, Co and Ni) of metal nitrides with the composition.

Table 1 Optimized lattice constants or inter-atomic distance of Fe (metal), Co (metal), Ni (metal) and N₂ gas molecule compared with observed ones, their calculated electronic energies, and magnetic moments.

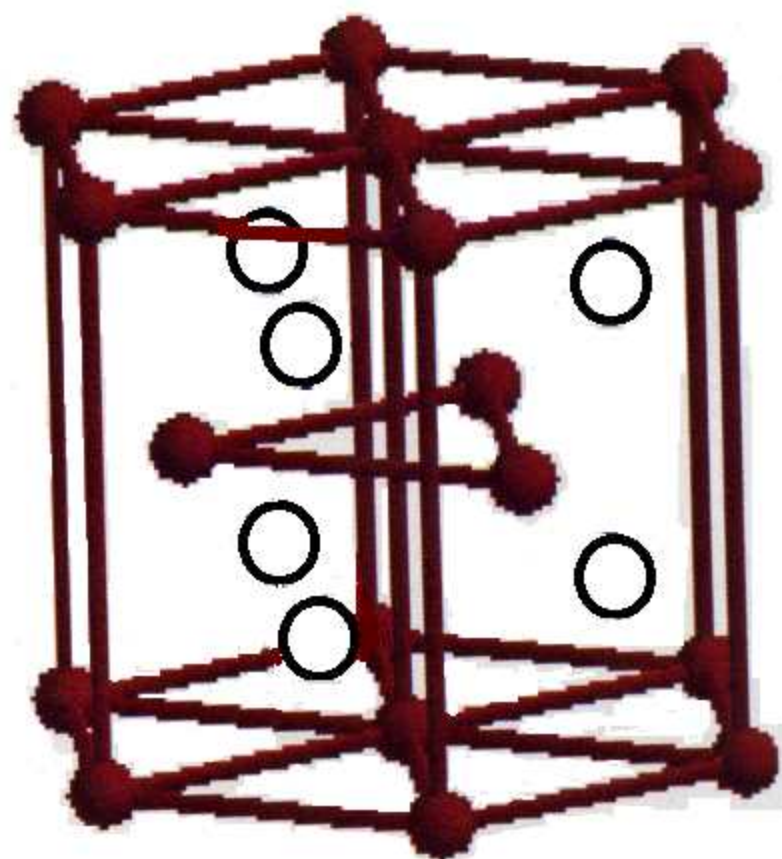
Table 2 Calculated electronic energies of optimized Me₄N (Me=Fe, Co or Ni), lattice constants, and their formation energies from metal and N₂ molecule and magnetic moments per 3d-atom.

Table 3 Calculated electronic energies of optimized Me₁₆N₂ with the α"-FeSi₂ type structure and Me₈N with the Ni₃₂Si₄ type structure (Me=Fe, Co or Ni).

Lattice constants, their formation energies from metal and N₂ molecule, and magnetic moments per 3d-atom are also given.

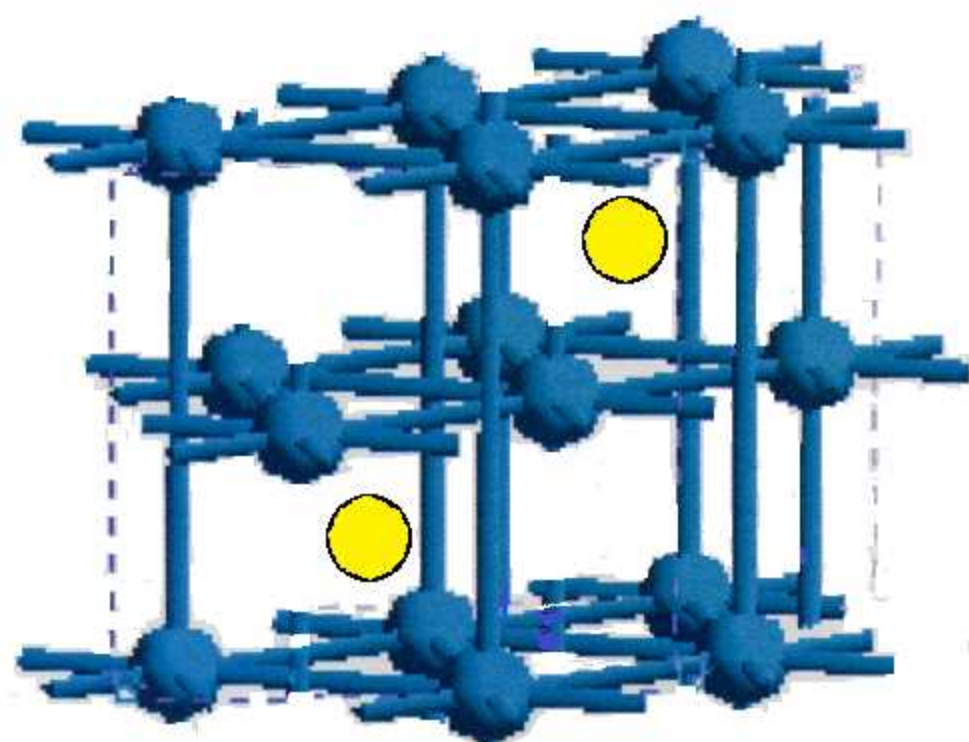
Table 4 Calculated electronic energies of optimized Me₆N₂ (Me=Fe, Co or Ni) with the, Ni₃N type structure, lattice constants, their formation energies from metal and N₂ molecule, and magnetic moments per 3d-atom.

(a) HCP lattice and its interstitial sites

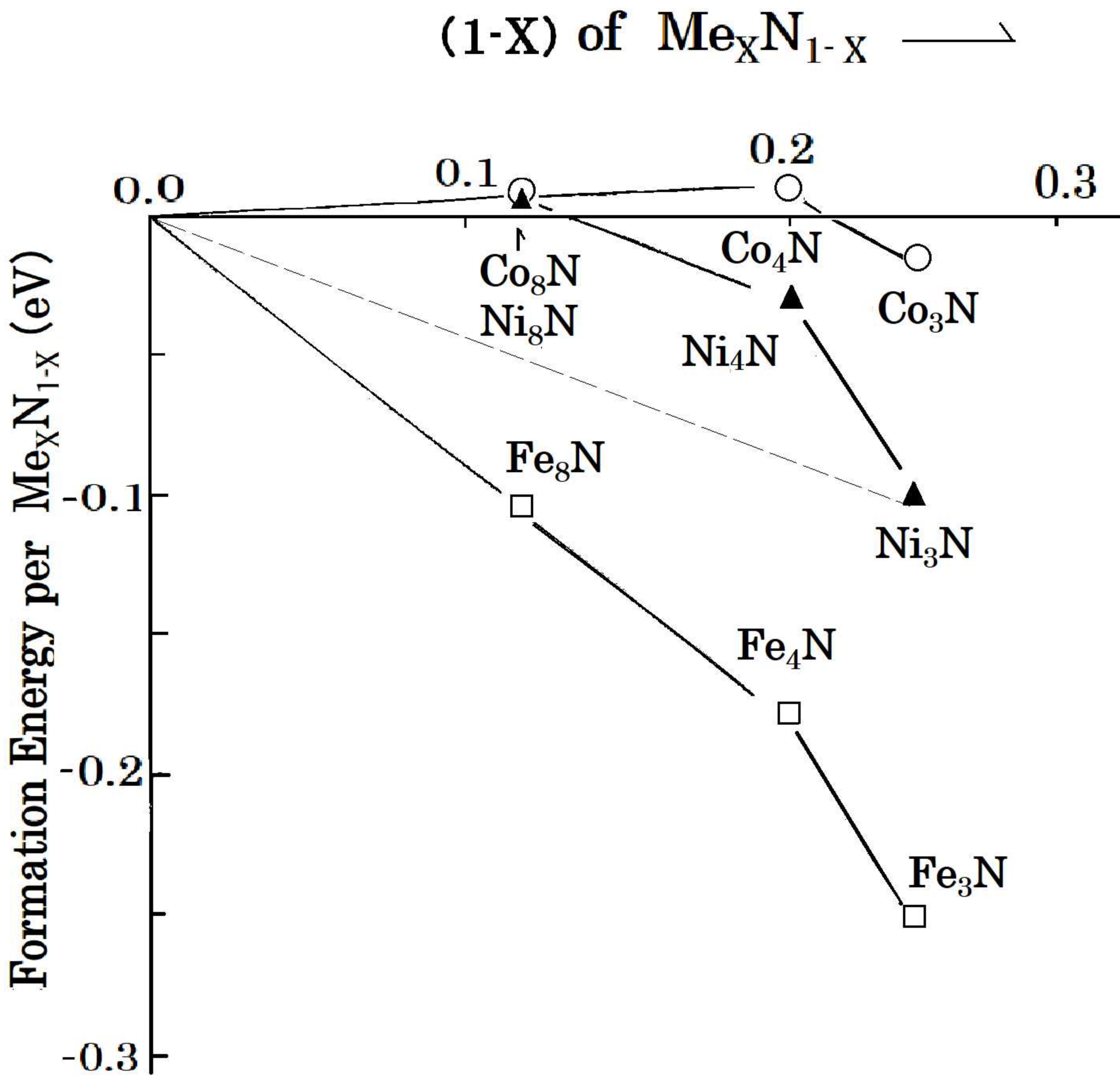


- Metal Atom (HCP Lattice)
- Interstitial Site

(b) Crystal structure of Ni₃N



- Ni
- N



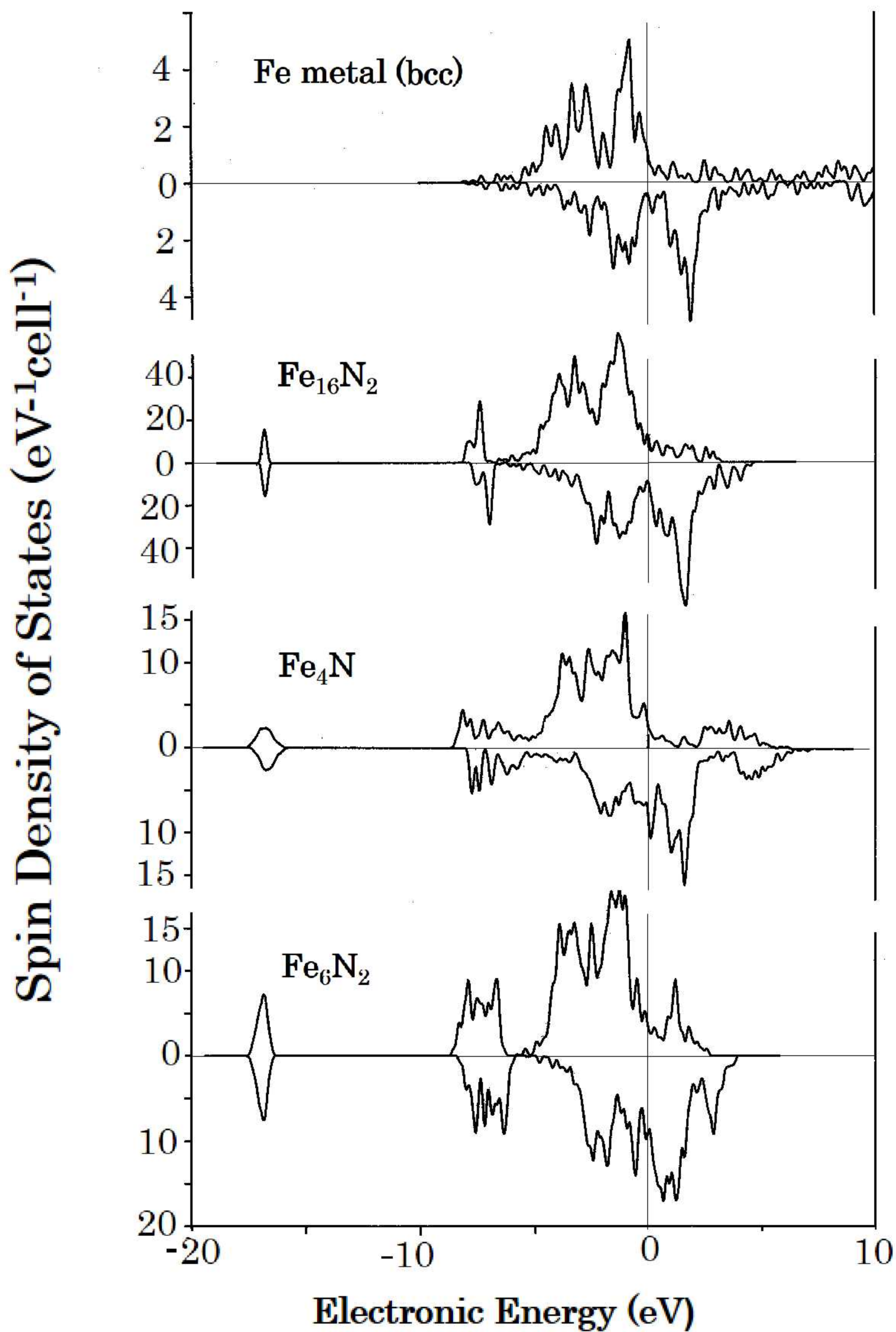


Fig. 4

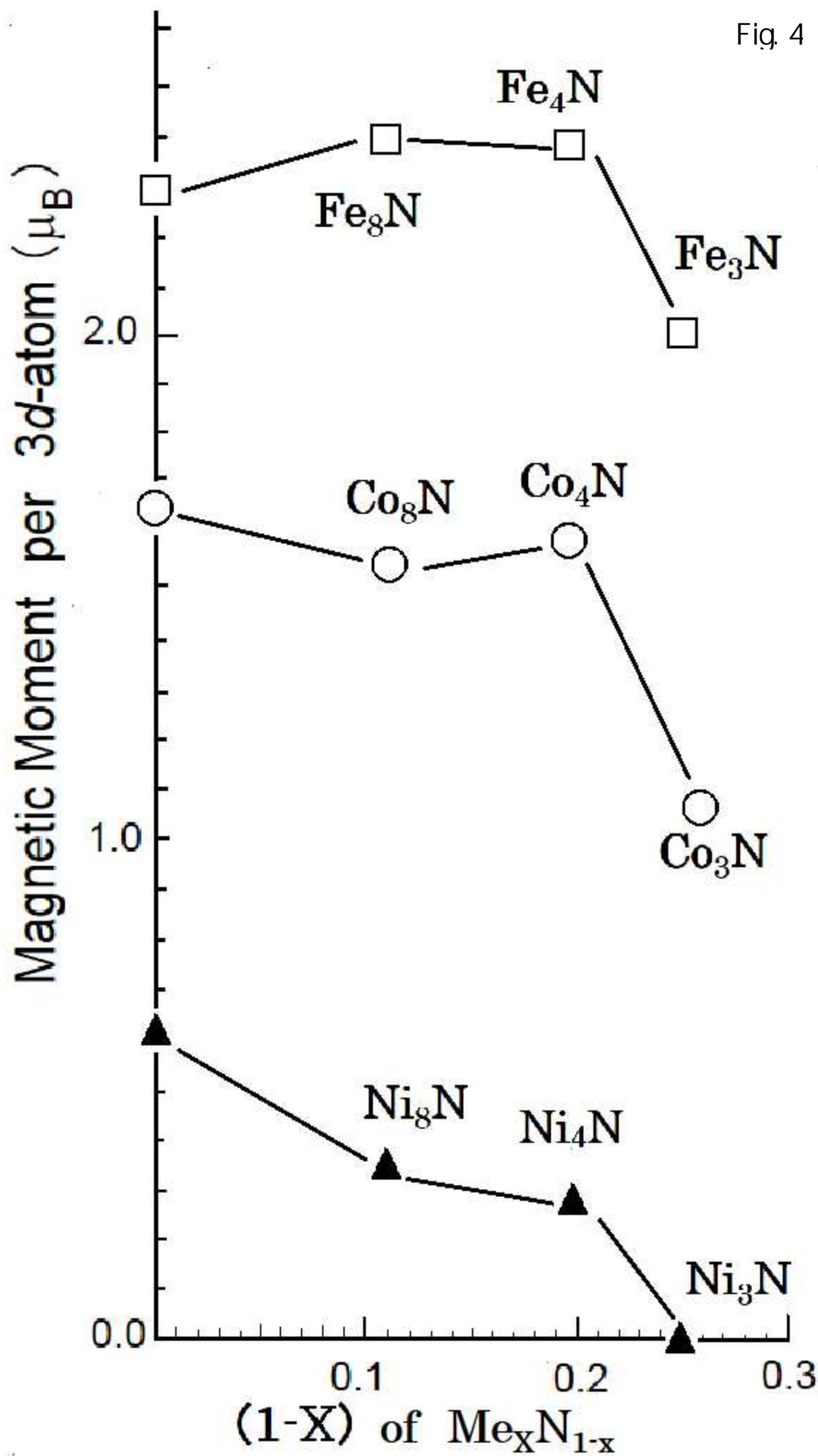


Table 1

Compound	Optimized Lattice Constants or Interatomic Distance <nm, deg> 【Observed value】	Magnetic Moment < μ_B > 【Observed value】	Calculated Total Electronic Energy for the Optimized Structure (eV)	Calculated Total Electronic Energy per atom (eV)
N ₂	0.1152 【0.1097】	0 【0】	-543.9973	-271.9987
Fe (bcc)	a=b=c=0.2450, $\alpha=\beta=\gamma=109.47$ 【a=b=c=0.2482, $\alpha=\beta=\gamma=109.47$ 】	2.31 【2.2】	-868.1636	-868.1636
Fe (fcc)	a=b=c=0.2437, $\alpha=\beta=\gamma=60$ 【a=b=c=0.2579 at 1190K】	0	-868.0103	-868.0103
	a=b=c=0.2549 $\alpha=\beta=\gamma=60^\circ$	2.57	-868.0101	-868.0101
Fe (hcp)	a=b=0.2464, c=0.3850, $\alpha=\beta=90, \gamma=120$ 【a=b=0.2465 c=0.4050 at 15GPa】	0	-1736.2418	-868.1209
Co (hcp)	a=b=0.2513, c=0.4072, $\alpha=\beta=90, \gamma=120$ 【a=b=0.2507, c=0.4069, $\alpha=\beta=90, \gamma=120$ 】	3.338/Co ₂ =1.67/Co ₁ 【1.7/Co ₁ 】	-2093.4390	-1046.7195
Co (fcc)	a=b=c=0.2511, $\alpha=\beta=\gamma=60$ 【a=b=c= 0.2506 at 696 K】	1.64 【1.75】	-1046.6993	-1046.6993
Ni (fcc)	a=b=c=0.2506, $\alpha=\beta=\gamma=60^\circ$ 【a=b=c=0.2492, $\alpha=\beta=\gamma=60$ 】	0.62 【0.62】	-1358.9228	-1358.9228

Table 2

Compound Space Group	Optimized Lattice Constants or Interatomic Distance (nm) 【Observed value】	Magnetic Moment (μ_B)	Calculated Total Electronic Energy for the Optimized Structure (eV)	Formation Energy for the Optimized Structure (eV) 【Reference State】
Fe_4N	a=0.3763 【0.3795】	9.555 =2.39/Fe	-3745.5480	-0.8949 【bcc Fe and N_2 gas】
Co_4N	a=0.3776 【0.374】	6.549 =1.64/Co	-4458.8265	+0.0502 【hcp Co and N_2 gas】
Ni_4N	a=0.3755 【0.374】	1.133 =0.283/Ni	-5707.7799	-0.1400 【fcc Ni and N_2 gas】

Table 3

Compound (Assumed Crystal Structure)	Optimized Lattice Constants or Interatomic Distance (nm) 【Observed value】	Magnetic Moment (μ_B)	Calculated Total Electronic Energy for the Optimized Structure (eV)	Formation Energy for the Optimized Structure (eV) 【Reference State】
Fe_{16}N_2 (body-centered tetragonal) I4/mmm	a= b=0.5641, c=0.6172 【a = b = 0.572 , c=0.629】	38.20 =2.39/Fe	-14436.4879	-1.8728 【bcc Fe and N ₂ gas】
Fe_8N_1 (reduced from fcc-Fe ₃₂ N ₄)	a=0.5159	17.42 =2.18/Fe	-7217.5672	-0.2596 【bcc Fe and N ₂ gas】
Co_{16}N_2 (body-centered tetragonal) I4/mmm	a=b= 0.5164 c=0.7251	24.54 =1.53/Co	-17291.3714	+0.1379 【hcp Co and N ₂ gas】
Co_8N_1 (reduced from fcc-Co ₃₂ N ₄)	a=0.5147	11.79 =1.47/Co	-8646.6427	+0.1119 【hcp Co and N ₂ gas】
Ni_{16}N_2 (body-centered tetragonal) I4/mmm	a=b=0.5161 c=0.7251	5.737 =0.36/Ni	-22286.6263	+0.1357 【fcc Ni and N ₂ gas】
Ni_8N_1 (reduced from fcc-Ni ₃₂ N ₄)	a=0.5146 【0. 5126】	2.037 =0.26/Ni	-11143.2259	+0.1552 【fcc Ni and N ₂ gas】

Table 4

Compound	Optimized Lattice Constants (nm)	Magnetic Moment (μ_B)	Calculated Total Electronic Energy for the Optimized Structure (eV)	Formation Energy for the Optimized Structure (eV) 【Reference State】
Fe_6N_2	a= b=0.4646, c=0.4310	12.26 =2.04/Fe	-5755.00814	-2.0292 【bcc Fe and N_2 gas】
Co_6N_2	a=b= 0.4636, c=0.4323	6.24 =1.04/Co	-6824.4078	-0.09347 【hcp Co and N_2 gas】
Ni_6N_2	a=b= 0.4646, c=0.4307	0.0	-8698.3295	-0.7954 【fcc Ni and N_2 gas】